SMGroup

SM Journal of Biomedical Engineering

Research Article

Fabrication of Conjugates Based on Poly (Ethylene Glycol) and Graphene Oxide for Antibacterial Wound Dressing Application

Lin Tan[1] and Jinlian Hu[1,2]*

[1]*Institute of Textiles and Clothing, The Hong Kong Polytechnic University, Hong Kong, China*
[2]*PolyU Shenzhen Base, Nanshan District, Shenzhen, China*

Article Information

Received date: Nov 20, 2015
Accepted date: Jan 27, 2016
Published date: Feb 05, 2016

***Corresponding author**

Jinlian Hu, PolyU Shenzhen Base, Nanshan District, Shenzhen, China, Email: jin-lian.hu@polyu.edu.hk

Keywords Graphene Oxide Grafts; Drug Carrier; Controlled Release

Abstract

Wound infection leading to the uneasy wound management is an outrageous problem which needs to be solved seriously. This work aims to fabricate one drug carrier system, and the loaded natural antibacterial agent can be released in a controlled and long-lasting manner, especially under the pH value of alkaline environment. The results show that the fabricated drug carrier, Poly (Ethylene Glycol) (PEG) grafted on Graphene Oxide (GO) (denoted as PEG-g-GO), can carry Berberine Chloride Hydrate (BCH) with high efficiency and then release it in a controlled way against different pH values. Furthermore, such BCH carrier can be easily coated on the cotton fabric, and finally the functional fabric may show potential to be applied as an antibacterial wound dressing to control the wound infection and thus erase the unpleasant odour.

Introduction

In order for effectively transferring the drugs into the target sites, numerous smart drug carriers have been developed and applied in biomedical fields through the popular forms of micelle, hydrogel, nanofibrous mats, bulk membrane, fabric, sponge and particle [1,2]. Additionally, among the biomedical applications, wound dressing can be regarded as a typical platform to release the drugs or growth factors to the wound for better and accelerating recovery [3].

Currently, there are three main types of controlled-release medications, including pulse-release [4], extended-release [5] and delayed-release [6]. Each type of release shows individual mechanism and has been taken into particular applications. However, the extended-release is always a preferable one in virtue of its long-lasting functional performance on the target site, especially that the performance is dependent on the change of physiological conditions, such as pH value, temperature and ion concentration. For instance, the pH-triggered time-extended release can be applied for wound protection against bacterial infection [7].

Wound pH value has been demonstrated as a potent influential factor during the healing process, and an increased pH milieu from neutral to alkaline will lead to the bacterial colonization and thus a higher biofilm will be produced on the wound bed [8,9]. Additionally, unpleasant odours, such as putrescine and cadaverine, generated from wound bed are largely caused by the infection of anaerobic and aerobic bacteria [10]. In order to address such problem, the concept of a controlled and sustained release of antibacterial drug from one carrier has been intensively developed, and one of efficient strategies is to construct a formulation which is capable to deliver incorporated drugs in a pH-dependent manner, preferentially at predefined rates under alkaline condition, such as pH value around 9.0.

Graphene Oxide (GO) is a unique two-dimensional material and possesses many merits. It also has been utilized extensively in biomedical fields, and one of the prominent applications is to apply GO-based materials as nano-carriers to carry the drug, growth factor or gene through π-π stacking, hydrogen bonding interaction and electrostatic interaction, then the carried compounds can be released in a controlled way [11]. In addition, the chemical modification is a basic way to further improve the dispersity and decrease the toxicity of GO sheets, such as grafting with biocompatible Polyethylene Glycol (PEG) [12]. Berberine, a natural and main alkaloid of *Coptis chinensis*, has been studied as an adjuvant therapeutic agent for the prevention of biofilm-related infection [13]. In addition, berberine has shown several other pharmacologic properties, such as anti-inflammatory, antidiarrheal and antipyretic activities [14]. Currently, in order to reduce the abuse of antibiotics, applying such natural antibacterial product is a desirable alternative to prevent the microorganism infection.

OPEN ACCESS
ISSN: 2573-3702

How to cite this article Tan L and Hu J. Fabrication of Conjugates Based on Poly (Ethylene Glycol) and Graphene Oxide for Antibacterial Wound Dressing Application. SM J Biomed Eng. 2016; 2(1): 1005.

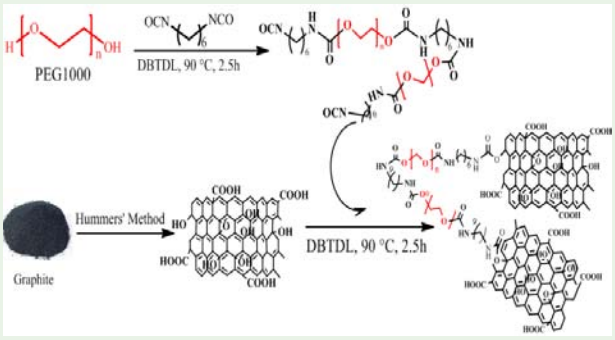

Figure 1: Schematic illustration of synthesis of GO and PEG-g-GO.

In this respect, PEG grafted on GO sheets was synthesized, and then the graft was applied to load berberine as the carrier. The release manner of berberine was investigated under near neutral and alkaline conditions. Also, in virtue of the pH-triggered release, the fabric coated with such berberine carrier may be recommended as a potential dressing to continuously prevent the bacteria infection for chronic wound recovery.

Experimental

Materials

Poly(Ethylene Glycol) (PEG, Mn=1000g/mol) was purchased from International Laboratory, USA, Hexamethylene Diisocyanate (HDI) and Dibutyltin Dilaurate (DBTDL) were purchased from Sigma Aldrich (USA). Berberine Chloride Hydrate (BCH, 98%, M_W=371.81) was purchased from Aladdin Com and used as received. Natural graphite powder, potassium permanganate and sodium nitrate were purchased from Unichem (Hong Kong). Other solvents and reagents were of analytical grade from local companies and used as received without further treatment.

Synthesis of PEG-*g*-GO

The synthesis map of PEG-*g*-GO is shown in Figure 1. Particularly, GO was synthesized from graphite powder based on Hummers' Method for first [15]; PEG was modified with excessive HDI so that isocyanate groups (-NCO) were naked to couple with GO sheets. Finally, PEG-*g*-GO was obtained by applying HDI as the linker. After stopping the reaction, the reaction resultant was poured inside a dialysis bag (molecular weight cut-off, MWCO of 8000 ~14000 DA) to remove the residual PEG, PEG-NCO and even smaller size of GO through dialysis against pure distilled water for one week. Finally, using air-drying method to obtain the final PEG-*g*-GO in a fume cupboard with a continuous air flow (Face Velocity: 450-500m/sec).

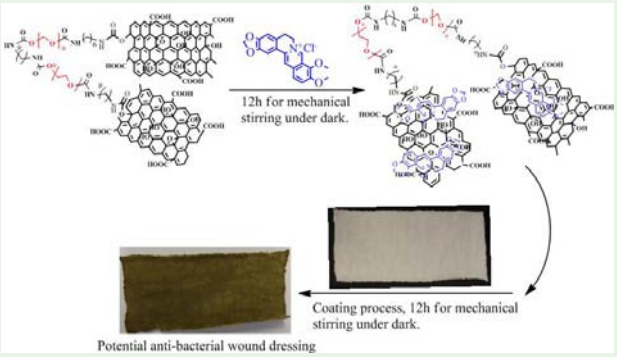

Figure 2: The process of BCH loading on PEG-g-GO carrier, and the subsequent coating on cotton fabric.

Loading BCH on PEG-*g*-GO

Firstly, the homogenous aqueous dispersion of PEG-*g*-GO was prepared with the concentration of 10 mg/mL, and then adding a calculated amount of BCH into the above PEG-*g*-GO solution. The weight ratio between BCH and PEG-*g*-GO was fixed at 1:2, meaning that the concentration of BCH in the final solution was 5 mg/ml. Then the complex was treated with mechanical stirring for a further 12 hours under dark. Finally, the complex was coated on the cotton fabric through the conventional operation (Figure 2). Before and after loading BCH, the size of PEG-*g*-GO and PEG-*g*-GO/BCH complex in the aqueous dispersion solution was investigated by applying one size analyzer (ZetaPlus Particle Sizing Analyzer, 90Plus/BI-MAS multi angle particle sizing instrument from Brookhaven instruments) with ten times scanning, and the size increment of PEG-*g*-GO after loading BCH was taken to confirm the successful loading.

Characterizations

The chemical structure of GO has been characterized in our previous study [16], and the structure of PEG-*g*-GO was confirmed by Fourier Transform Infrared (PerkinElmer Spectrum 100 FT-IR Spectrometer, USA) spectroscopy in the range of 650~4000 cm^{-1} at room temperature; Thermal decomposition was investigated by thermogravimetric analysis (Mettler Toledo TGA/DSC 1 Simultaneous Thermal analyser, Switzerland) with a heating scan from room temperature to 800 ℃ by the heating rate of 10 ℃/min, the flow rate of applied nitrogen gas was maintained at 50 mL/min, and the grafting ratio of PEG on GO was calculated according to the residue ratio of carbonization materials after pyrolysis.

BCH release from PEG-*g*-GO and accumulative calculation

The BCH loaded PEG-*g*-GO solution was distributed into separated tubes. Every small tube contained 1.5 mL solution, then using dialysis membrane (MWCO=3500 DA) to seal the opening of each tube for release investigation, and the size of circular release window for each tube was 1.0 cm in diameter. Subsequently, every sealed small tube was inversely placed inside a larger tube containing 15 mL phosphate-buffered saline buffer with two pH values (pH 7.41 and pH 9.00), and finally all the tubes were incubated in a shaking platform under 36.5±0.5 ℃.

In the course of release, 2.0 mL of the solution was withdrawn and an equal amount of the fresh PBS was replaced at the specific time intervals. The amount of released BCH was determined by a UV/VIS Spectrophotometer (PE Spectrometer Lambda 18) at the maximal absorption peak. Additionally, the linear calibration curves of BCH under different pH values were obtained through one series of standard BCH solutions with the concentration range of 0-0.025 mg/mL.

Results and Discussion

FT-IR characterization and thermal property investigation

The structure of synthesized PEG-*g*-GO was characterized by FI-IR spectroscopy, and the corresponding spectra of GO and PEG

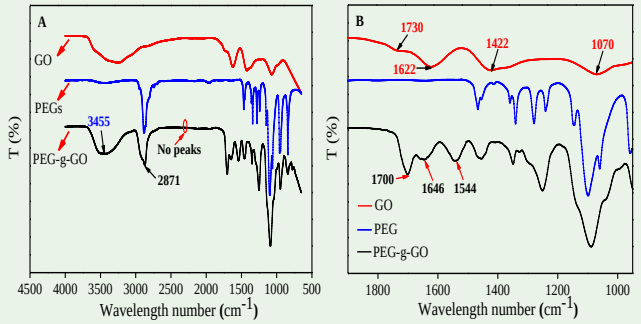

Figure 3: FT-IR (A) and TGA (B) analysis of GO, PEG and PEG-g-GO.

were applied as the control. As the curves shown in Figure 3(A), the obvious peaks on ~3455 cm^{-1} and ~2871 cm^{-1} of PEG-*g*-GO indicate the existence of a large number of -OH groups and C-H bonds which are mainly derived from GO and PEG, respectively. No peak around 2270 cm^{-1} can be found that suggests the reaction with -NCO groups thoroughly happened. Particularly, the typical peaks lie on ~1730 cm^{-1}, ~1622 cm^{-1}, ~1422 cm^{-1} and ~1045 cm^{-1} are corresponding to the vibration of C=O, C=C, O-H and C-O groups of GO, respectively [17,18]; Additionally, the new-forming characteristic peaks of ~1700 cm^{-1}, ~1646 $cm^{-1}$and 1544 cm^{-1} can be ascribed to the strong stretching vibration of carbamate esters derived from the peak of ~1730 cm^{-1}, amide I and amide II stretching vibration, respectively [19] (Figure 3(B)). In general, FI-IR spectra demonstrate that PEG was successfully grafted on GO through the linker of HDI.

Figure 4(A) shows the pyrolysis behavior of GO, PEG and PEG-*g*-GO. Before 120 ℃, the weight loss of three materials is attributed to the absorbed free water, and among them, GO shows the most significant loss (around ~20 wt%), indicating that the synthesized GO has high an oxidation degree so that it can absorb more water regarding as a surfactant. After 120 ℃, GO shows an another rapid thermal degradation process which is derived from the loss of oxygen-containing functional groups, and the Maximum Degradation Temperature (MDT) is around 197.3 ℃ [20]. While PEG and PEG-*g*-GO mainly show one typical weight loss process, and the MDT of PEG and PEG-*g*-GO are 385.3 ℃ and 393.2 ℃, respectively (Figure 4(B)), and such result can suggest that (1) more PEG in weight constituting the PEG-*g*-GO, and (2) GO shows heat barrier affect so that PEG-*g*-GO has a slight higher thermal stability [21]. Hence, according to the weight ratio (W_r) of GO, PEG and PEG-*g*-GO on 120 ℃ and the corresponding final residual nonvolatile carbonaceous materials after the heating process, the grafting ratio (A) of PEG on GO sheets by mass is around 82.0% calculated through the following equation.

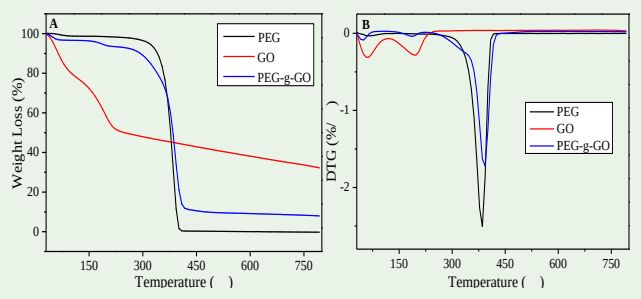

Figure 4: TGA and DTG curves of GO, PEG and PEG-g-GO.

$$(W_{r120-PEG} - W_{r800-PEG}) \times A + (W_{r120-GO} - W_{r800-GO}) \times (1 - A) = (W_{r120-PEG-g-GO} - W_{r800-PEG-g-GO})$$

where $W_{r120\text{-}PEG}$, $W_{r800\text{-}PEG}$, $W_{r120\text{-}GO}$, $W_{r800\text{-}GO}$, $W_{r120\text{-}PEG\text{-}g\text{-}GO}$ and $W_{r120\text{-}PEG\text{-}g\text{-}GO}$ are 98.7%, 0.0%, 77.3%, 33.0%, 96.6% and 7.7% according to the curves in Figure 4(A), respectively.

BCH loading investigation

As the loading process illustrated in Figure 2, thanks to the unique structural features of BCH, including quaternary ammonium base, isoquinoline ring, benzodioxole and methoxyl, BCH can possibly interact with PEG-*g*-GO through the π-π stacking, hydrophobic effect, hydrogen bonding and electrostatic adsorption interaction.

According to the size results shown in Figure 5, the size of PEG-*g*-GO is around 946.3±20.5 nm before BCH loading, and PEG-*g*-GO kept stable in the aqueous solution and shows almost the same size of 903.3±16.3 nm after loading process. However, with the incorporation of BCH, the size of PEG-*g*-GO/BCH significantly increases to 1390.2±30.7 nm. Therefore, it can indicate that PEG-*g*-GO successfully carried BCH and formed the stable complex during the loading process.

Release behavior observation

As the full-scanning screen shown in Figure 6(A), BCH has three typical absorption peaks, and the absorption wavelength around 343 nm in virtue of π-π* transitions of the isoquinolin structure is the most distinguished one, hence, such peak was chosen to prepare the standard curves and then investigate the accumulative release of BCH by the function of time. Figure 6(B) shows the two prepared calibration curves with desirable linearity (R^2=0.9935~0.9999) under pH=7.41 and 9.00, and there is a little difference between the two curves which can be attributed to the conditioned pH values.

The accumulative release of BCH under two different conditions was calculated according to the above standard curves separately. Firstly, at the initial stage 1 (within 24 h), the release behavior under two pH value conditions was almost similar, and about 20% BCH was released from PEG-*g*-GO matrix. However, afterward, the release behavior began to be obvious different (stage 2). The release under pH=7.41 kept fast, but that under pH=9.00 became lower, and the three-day accumulative release of BCH was up to 51.3±1.4% and 40.1±2.2% under pH=7.41 and 9.00, respectively (Figure 7(left)). After one week investigation, the carried BCH was released in a higher ratio of 91.4±1.7% under pH=7.41 and a significant lower release content of 71.3±0.5% under the alkaline environment. Generally, near neutral and alkaline conditions yielded individual effects on the release of BCH from the carrier of PEG-*g*-GO. Also, such pH-triggered release

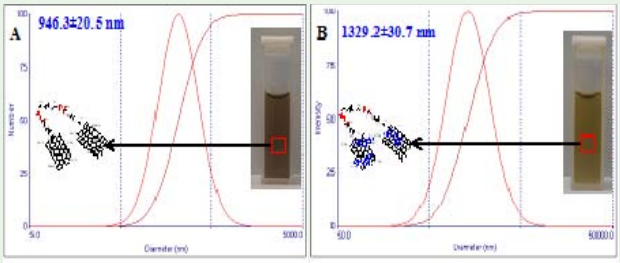

Figure 5: Particle size analysis of before (A) and after (B) loading BCH. Notes: The comparison one keeps the size of 903.3±16.3 nm without loading BCH.

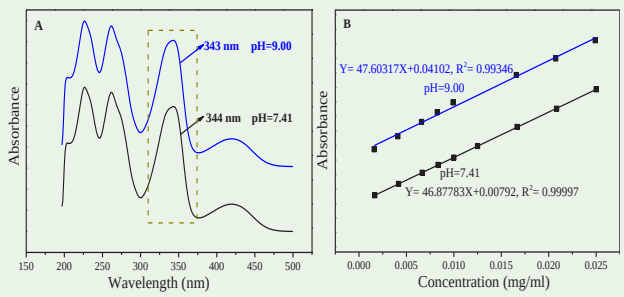

Figure 6: Standard curves of BCH under the pH value of 7.41 and 9.00.

can perform in a controlled and long-lasting manner, especially under alkaline condition of pH=9.00 compared with that manner under near neutral condition, and no obvious initial burst release can be found.

Figure 7(right) shows the proposed release mechanism against near neutral and alkaline conditions. In short, different pH conditions affect the interactions between BCH and carrier of PEG-*g*-GO. Unlike other drugs, such as doxorubicin hydrochloride [22] and SN38 (a camptothecin analogue) [23], the main interactions between them and GO sheets include π-π stacking and hydrogen bonding. However, electrostatic adsorption is also another prominent interaction existing between BCH and PEG-*g*-GO due to the presence of quaternary ammonium base structure [24].

Particularly, there are four main states of BCH lying inside PEG-*g*-GO carrier, including the uncontrolled state and the other states maintained through the interaction of π-π stacking, hydrogen bonding and electrostatic adsorption (a). Under near neutral condition, loose electrostatic interaction, π-π stacking and tight hydrogen bonding exist, and BCH releases in the conventional controlled way, mainly depends on the solvent competition and solute diffusion (b). In contrast, under alkaline environment, both quaternary ammonium base of BCH and carboxyl groups on GO sheet edge will be further ionized, thus the strong electrostatic adsorption happens. However, partial hydrogen bonds between BCH and GO will be weakened and then the matrix becomes loose during the ionization process [22] (c). In general, PEG-*g*-GO matrix can carry BCH more tightly under alkaline condition, therefore, BCH releases in a faster way under near neutral condition. Finally, because of the characteristic of pH-triggered release, the antibacterial fabric coated with such PEG-*g*-GO/BCH complex may possibly provide sustainable protection from infection, and thus prevent the generation of unpleasant odour.

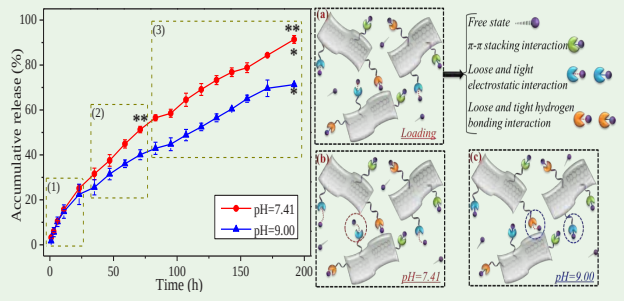

Figure 7: Release behavior of BCH from PEG-g-GO carrier (left), and the corresponding proposed release mechanism of BCH under neutral and alkaline conditions (right).

Conclusion

In this study, we successfully developed a drug carrier, PEG-*g*-GO, to load the natural antibacterial agent, BCH. More importantly, PEG-*g*-GO can control the release of BCH in a pH-triggered and long-lasting manner. Therefore, the cotton fabric coated with such PEG-*g*-GO/BCH may potentially provide sustainable protection from bacterial infection under alkaline condition, and thus to avoid the generation of unpleasant wound odour when applied as a wound dressing. Furthermore, the developed drug carrier loading with BCH can be applied in other biomedical fields, such as diarrhea, cardiovascular diseases and anti-hyperglycemia.

Acknowledgement

This work was sponsored by National Key Technology R&D Program project of China (2012BAI17B00: 2012B2012BAI17B06), Shenzhen Biological, New Energy, New Material Industry Development Special Funds (JC201104210132A).

References

1. Mansour HM, Sohn M, Al-Ghananeem A, DeLuca PP. Materials for pharmaceutical dosage forms: molecular pharmaceutics and controlled release drug delivery aspects. International journal of molecular sciences. 2010; 11: 3298-3322.
2. Liechty WB, Kryscio DR, Slaughter BV, Peppas NA. Polymers for drug delivery systems. Annual review of chemical and biomolecular engineering. 2010; 1: 149-173.
3. Tan L, Hu JL, Zhao HF. Design of bilayered nanofibrous mats for wound dressing using an electrospinning technique. Materials Letters. 2015; 156: 46-49.
4. Biswas N, Guha A, Sahoo RK, Kuotsu K. Pulse release of doxazosin from hydroxyethylcellulose compression coated tablet: Mechanistic and in vivo study. International journal of biological macromolecules. 2015; 72: 537-543.
5. Han N, Johnson J, Lannutti JJ, Winter JO. Hydrogel-electrospun fiber composite materials for hydrophilic protein release. Journal of Controlled Release. 2012; 158: 165-170.
6. Aw MS, Addai-Mensah J, Losic D. Polymer micelles for delayed release of therapeutics from drug-releasing surfaces with nanotubular structures. Macromolecular bioscience. 2012; 12: 1048-1052.
7. Liu H, Zhen M, Wu R. Ionic-strength and pH-responsive Poly [acrylamide-co-(maleic acid)] hydrogel nanofibers. Macromolecular Chemistry and Physics. 2007; 208: 874-880.
8. Hostacka A, Ciznar I, Stefkovicova M. Temperature and pH affect the production of bacterial biofilm. Folia microbiologica. 2010; 55: 75-78.
9. Schneider LA, Korber A, Grabbe S, Dissemond J. Influence of pH on wound-healing: a new perspective for wound-therapy?. Archives of dermatological research. 2007; 298: 413-420.
10. Fleck C. Palliative dilemmas: wound odour. Wound Care Canada. 2006; 4: 10-14.
11. Chung C, Kim YK, Shin D, Ryoo SR, Hong BH, Dal-Hee Min. Biomedical applications of graphene and graphene oxide. Accounts of chemical research. 2013; 46: 2211-2224.
12. Wen HY, Dong C, Dong H, Shen A, Xia W, Cai X, et al. Engineered redox-responsive peg detachment mechanism in pegylated nano-graphene oxide for intracellular drug delivery. Small. 2012; 8: 760-769.
13. Wang XQ, Yao X, Zhu ZA, Tang T, Dai K, Sadovskaya I, et al. Effect of berberine on Staphylococcus epidermidis biofilm formation. International journal of antimicrobial agents. 2009; 34: 60-66.
14. Lin YH, Lin JH, Chou SC, Chang SJ, Chung CC, Chen YS, et al. Berberine-

loaded targeted nanoparticles as specific Helicobacter pylori eradication therapy: in vitro and in vivo study. Nanomedicine. 2015; 10: 57-71.

15. Salavagione HJ, Gomez MA, Martínez G. Polymeric modification of graphene through esterification of graphite oxide and poly (vinyl alcohol). Macromolecules. 2009; 42: 6331-6334.

16. Tan L, Gan L, Hu JL, Zhu Y, Han JP. Functional shape memory composite nanofibers with graphene oxide filler. Composites Part A: Applied Science and Manufacturing. 2015; 76: 115-123.

17. Yang T, Liu LH, Liu JW, Chen ML, Wang JH. Cyanobacterium metallothionein decorated graphene oxide nanosheets for highly selective adsorption of ultra-trace cadmium. Journal of Materials Chemistry. 2012; 22: 21909-21916.

18. Wang X, Song L, Yang H, Xing W, Kandola B, et al. Simultaneous reduction and surface functionalization of graphene oxide with POSS for reducing fire hazards in epoxy composites. Journal of Materials Chemistry. 2012; 22: 22037-22043.

19. Stankovich S, Piner RD, Nguyen ST, Ruoff RS. Synthesis and exfoliation of isocyanate-treated graphene oxide nanoplatelets. Carbon. 2006; 44: 3342-3347.

20. Wu T, Wang X, Qiu H, Gao J, Wang W, Yu Liu. Graphene oxide reduced and modified by soft nanoparticles and its catalysis of the Knoevenagel condensation. Journal of Materials Chemistry. 2012; 22: 4772-4779.

21. Bao C, Guo Y, Song L, Hu Y. Poly (vinyl alcohol) nanocomposites based on graphene and graphite oxide: a comparative investigation of property and mechanism. Journal of Materials Chemistry. 2011; 21: 13942-13950.

22. Yang XY, Zhang X, Liu Z, Ma Y, Huang Y, Chen Y. High-efficiency loading and controlled release of doxorubicin hydrochloride on graphene oxide. The Journal of Physical Chemistry C. 2008; 112: 17554-17558.

23. Liu Z, Robinson JT, Sun X, Dai H. PEGylated nanographene oxide for delivery of water-insoluble cancer drugs. Journal of the American Chemical Society. 2008; 130: 10876-10877.

24. Yu D, Ruan P, Meng Z, Zhou J. The structure-dependent electric release and enhanced oxidation of drug in graphene oxide-based nanocarrier loaded with anticancer herbal drug berberine. Journal of pharmaceutical sciences. 2015; 104: 2489-2500.